

## BULLET CLUSTER: A CHALLENGE TO $\Lambda$ CDM COSMOLOGY

JOUNGHUN LEE<sup>1</sup> AND EIICHIRO KOMATSU<sup>2</sup>

<sup>1</sup> Department of Physics and Astronomy, FPRD, Seoul National University, Seoul 151-747, Republic of Korea; [jounghun@astro.snu.ac.kr](mailto:jounghun@astro.snu.ac.kr)

<sup>2</sup> Texas Cosmology Center and Department of Astronomy, The University of Texas at Austin, 1 University Station, C1400 Austin, TX 78712, USA  
 Received 2010 March 3; accepted 2010 May 20; published 2010 June 25

### ABSTRACT

To quantify how rare the bullet-cluster-like high-velocity merging systems are in the standard  $\Lambda$  cold dark matter (CDM) cosmology, we use a large-volume ( $27 h^{-3} \text{ Gpc}^3$ ) cosmological  $N$ -body MICE simulation to calculate the distribution of infall velocities of subclusters around massive main clusters. The infall velocity distribution is given at  $(1-3)R_{200}$  of the main cluster (where  $R_{200}$  is similar to the virial radius), and thus it gives the distribution of realistic initial velocities of subclusters just before collision. These velocities can be compared with the initial velocities used by the non-cosmological hydrodynamical simulations of 1E0657-56 in the literature. The latest parameter search carried out by Mastropietro & Burkert has shown that an initial velocity of  $3000 \text{ km s}^{-1}$  at about  $2R_{200}$  is required to explain the observed shock velocity, X-ray brightness ratio of the main and subcluster, X-ray morphology of the main cluster, and displacement of the X-ray peaks from the mass peaks. We show that such a high infall velocity at  $2R_{200}$  is incompatible with the prediction of a  $\Lambda$ CDM model: the probability of finding  $3000 \text{ km s}^{-1}$  in  $(2-3)R_{200}$  is between  $3.3 \times 10^{-11}$  and  $3.6 \times 10^{-9}$ . A lower velocity,  $2000 \text{ km s}^{-1}$  at  $2R_{200}$ , is also rare, and moreover, Mastropietro & Burkert have shown that such a low initial velocity does not reproduce the X-ray brightness ratio of the main and subcluster or morphology of the main cluster. Therefore, we conclude that the existence of 1E0657-56 is incompatible with the prediction of a  $\Lambda$ CDM model, unless a lower infall velocity solution for 1E0657-56 with  $\lesssim 1800 \text{ km s}^{-1}$  at  $2R_{200}$  is found.

**Key words:** cosmology: theory – large-scale structure of universe – methods: statistical

### 1. INTRODUCTION

The bow shock in the merging cluster 1E0657-57 (also known as the “bullet cluster”) observed by *Chandra* indicates that the subcluster (found by Barrena et al. 2002) moving through this massive ( $10^{15} h^{-1} M_{\odot}$ ) main cluster creates a shock, and the shock velocity is as high as  $4700 \text{ km s}^{-1}$  (Markevitch et al. 2002; Markevitch 2006). A significant offset between the distribution of X-ray emission and the mass distribution has been observed (Clowe et al. 2004, 2006; Markevitch et al. 2004), also indicating a high-velocity merger with gas stripped by ram pressure.

Several groups have carried out detailed investigations of the physical properties of 1E0657-57 using non-cosmological hydrodynamical simulations (Takizawa 2005, 2006; Milosavljević et al. 2007; Springel & Farrar 2007; Mastropietro & Burkert 2008). One of the key input parameters for all of these simulations is the *initial velocity* of the subcluster, which is usually given at somewhere near the virial radius of the main cluster.

An interesting question is whether the existence of such a high-velocity merging system is expected in a  $\Lambda$  cold dark matter ( $\Lambda$ CDM) universe. Hayashi & White (2006) were the first to calculate the likelihood of subcluster velocities using the Millennium Run simulation (Springel et al. 2005). As the volume of the Millennium Run simulation is limited to  $(0.5 h^{-1} \text{ Gpc})^3$ , there are only five cluster-size halos with  $M_{200} > 10^{15} h^{-1} M_{\odot}$ , and one cluster with  $M_{200} > 2 \times 10^{15} h^{-1} M_{\odot}$  at  $z = 0.28$  (close to the redshift of 1E0657-57,  $z = 0.296$ ). Therefore, Hayashi & White (2006) had to extrapolate their results for  $M_{200} > 10^{14} h^{-1} M_{\odot}$  assuming that the likelihood of finding the bullet-cluster systems scales with  $V_{\text{sub}}/V_{200}$ , where  $V_{\text{sub}}$  is the subcluster velocity in the rest frame of the main cluster, and  $V_{200} = (GM_{200}/R_{200})^{1/2}$ . Here,  $R_{200}$  is the radius within which the mean mass density is 200 times the critical density of the universe, and  $M_{200}$  is the mass enclosed within  $R_{200}$ .

While Hayashi & White (2006) concluded that the existence of 1E0657-57 is consistent with the standard  $\Lambda$ CDM cosmology, this conclusion was later challenged by Farrar & Rosen (2007) who showed that, once an updated mass of the main cluster of 1E0657-57 is taken into account, the probability of finding 1E0657-57 is as low as  $10^{-7}$ . This conclusion still relies on the extrapolation of the likelihood derived for  $M_{200} > 10^{14} h^{-1} M_{\odot}$ .

As the probability of finding high-velocity merging systems decreases exponentially with velocities, an accurate determination of the *subcluster velocity*, rather than the shock velocity, is crucial. Milosavljević et al. (2007) and Springel & Farrar (2007) used hydrodynamical simulations to show that the subcluster velocity can be significantly lower than the shock velocity (which is  $4700 \text{ km s}^{-1}$ ). Milosavljević et al. (2007) found that the subcluster velocity can be  $4050 \text{ km s}^{-1}$ , whereas Springel & Farrar (2007) found that it can be as low as  $2700 \text{ km s}^{-1}$ . Mastropietro & Burkert (2008) showed that the subcluster velocity of  $3100 \text{ km s}^{-1}$  best reproduces the X-ray data of 1E0657-57.

These varying results are in part due to the varying assumptions about the initial velocity given to the subcluster at the beginning of their hydrodynamical simulations: Milosavljević et al. (2007) used zero relative velocity between the main cluster and subcluster at an initial separation of 4.6 Mpc (which is two times  $R_{200}$  of the main cluster, 2.3 Mpc). The velocity is about  $1600 \text{ km s}^{-1}$  at a separation of 3.5 Mpc ( $\simeq 1.5 R_{200}$ ); Springel & Farrar (2007) used an initial velocity of  $2057 \text{ km s}^{-1}$  when the separation was 3.37 Mpc ( $\simeq 1.5 R_{200}$ ); and Mastropietro & Burkert (2008) explored various initial velocities such as  $2057 \text{ km s}^{-1}$  at the initial separation of 3.37 Mpc and 2000, 3000, and  $5000 \text{ km s}^{-1}$  at the initial separation of 5 Mpc ( $\simeq 2.2 R_{200}$ ). Mastropietro & Burkert (2008) found that the simulation run with an initial velocity of  $3000 \text{ km s}^{-1}$  best reproduces the X-ray data.

<sup>3</sup> M. Milosavljević (2010, private communication). All velocities quoted throughout this paper are calculated in the rest frame of the main cluster.

In this paper, we demonstrate that the initial velocities used by Milosavljević et al. (2007) and Springel & Farrar (2007) are consistent with the prediction of a  $\Lambda$ CDM model, but those of Mastropietro & Burkert (2008) at 5 Mpc are not. The simulations of Milosavljević et al. (2007) and Springel & Farrar (2007) do not reproduce details of the X-ray and weak lensing data of 1E0657-57, and Mastropietro & Burkert (2008) argue that one needs an initial velocity of  $3000 \text{ km s}^{-1}$  to explain the data. If this is true, the existence of 1E0657-57 is incompatible with the prediction of a  $\Lambda$ CDM model.

## 2. FINDING CLUSTERS OF CLUSTERS IN SIMULATION

As high-velocity systems are rare, it is crucial to use a large-volume simulation to derive a reliable probability distribution. The previous study is somewhat inconclusive due to the limited volume of the Millennium Run simulation ( $0.5 h^{-1} \text{ Gpc}^3$ ). We calculate the probability of finding bullet-like systems using a simulation with substantially larger volume ( $3 h^{-1} \text{ Gpc}^3$ ).

We use the publicly available simulated dark matter halo catalogs at  $z = 0$  and  $0.5$ , which are constructed from the largest-volume  $N$ -body Marenstrum Institut de Ciències de l'Espai (MICE) simulations (Crocce et al. 2010). They used the publicly available GADGET-2 code (Springel 2005), with the cosmological parameters of  $\Omega_m = 0.25$ ,  $\Omega_\Lambda = 0.75$ ,  $\Omega_b = 0.044$ ,  $h = 0.7$ ,  $n_s = 0.95$ , and  $\sigma_8 = 0.8$ . These numbers are consistent with those derived from the seven-year data of the Wilkinson Microwave Anisotropy Probe (Komatsu et al. 2010).

The MICE simulation that we shall use in this paper has a particle mass of  $M_{\text{par}} = 23.42 \times 10^{10} h^{-1} M_\odot$  and a linear box size of  $L_{\text{box}} = 3072 h^{-1} \text{ Mpc}$ . The standard friends-of-friends (FoF) algorithm (Davis et al. 1985) with a linking length parameter of  $b = 0.2$  was employed to find the cluster halos from the distribution of  $2048^3$  dark matter particles. See Fosalba et al. (2008) and Crocce et al. (2010) for a detailed description of the MICE simulations and the halo-identification procedure.

The halos identified in the MICE simulation contain at least 143  $N$ -body particles. The derived halo catalog contains the center-of-mass positions ( $\mathbf{X}$ ) and velocities ( $\mathbf{V}$ ) of halos, as well as the number of particles in each halo ( $N_{\text{par}}$ ). Note that the number of particles in each halo has been corrected for the known systematic effect of the FoF algorithm, using  $N_{\text{par}}^{\text{corr}} = N_{\text{par}}(1 - N_{\text{par}}^{-0.6})$  (Warren et al. 2006; Crocce et al. 2010).

The mass of each halo is calculated as  $N_{\text{par}}$  times the mass of each particle,  $M_{\text{par}}$ . The mass of halos identified by FoF with a linking length of  $0.2$  approximately corresponds to  $M_{200}$ , i.e., the mass within  $R_{200}$ , within which the overdensity is 200 times the critical density of the universe at a given redshift,  $M_{200} = \frac{4\pi}{3} [200\rho_c(z)] R_{200}^3$ . It is, however, known that the FoF mass tends to be larger than  $M_{200}$ , especially for high-mass clusters which are less concentrated (Lukić et al. 2009). As a result,  $R_{200}$  we quote in this paper may be an overestimate.

The difference between the FoF mass and  $M_{200}$  decreases as the number of particles per halo,  $N_{\text{par}}$ , increases (Lukić et al. 2009). For the main halo masses of our interest,  $M_{\text{main}} \geq 0.5 \times 10^{15} h^{-1} M_\odot$ , the average value of  $N_{\text{par}}$  is 3355 and 3160 at  $z = 0$  and  $0.5$ , respectively. Using this, we estimate that, on average, our  $R_{200}$  may be 10% too large. This error is insignificant for our purpose. Moreover, as correcting this error strengthens our conclusion by making the probability of finding high-velocity subclusters even smaller, we shall ignore the difference between  $R_{200}$  and the radius estimated from the FoF mass.

**Table 1**  
Clusters of Clusters from the MICE Simulation

$z$	Number of Clusters	Number of Clusters of Clusters <sup>a</sup>	Mean Mass of Main Clusters
0	2.8 million	0.29 million	$1.3 \times 10^{14} h^{-1} M_\odot$
0.5	1.7 million	0.20 million	$1.1 \times 10^{14} h^{-1} M_\odot$

**Note.**

<sup>a</sup> A “cluster of clusters” is a group of cluster-size halos identified by the FoF algorithm. A useful picture is a massive cluster surrounded by many less massive clusters.

To find the “clusters of clusters” (i.e., groups of clusters with one massive main cluster surrounded by many less massive satellite clusters), we treat each cluster in the catalog as a particle and re-apply the FoF algorithm with a linking length of  $0.2$ . This time, the linking length of  $0.2$  means the length of  $0.2$  times  $L_{\text{box}}/(N_{\text{cl}})^{1/3}$ , where  $N_{\text{cl}}$  is the total number of clusters found in the simulation (2.8 and 1.7 million clusters at  $z = 0$  and  $0.5$ , respectively). Each cluster of clusters has the “main cluster,” or the most massive member of each cluster of clusters. All the other clusters are called “satellite clusters” or “subclusters.” Table 1 shows the total number of cluster-size halos found in the simulation, the number of clusters of clusters having at least two members, and the mean mass of main clusters. For each main cluster, we calculate  $R_{200}$  from its mass as  $R_{200} = [3M_{200}/(4\pi \times 200\rho_c(z))]^{1/3}$ . Most of the satellite clusters are located at  $r \gtrsim 2R_{200}$  from the main cluster, where  $r$  is the distance between the main cluster and its satellites.

## 3. DERIVING THE INFALL VELOCITY DISTRIBUTION

Our goal in this paper is to derive the distribution of infall velocities around the main clusters. To compare with the initial velocities used by the hydrodynamical simulations in the literature (Milosavljević et al. 2007; Springel & Farrar 2007; Mastropietro & Burkert 2008), we calculate the infall velocity distribution within  $(2-3)R_{200}$  (Mastropietro & Burkert 2008), at  $1.5R_{200}$  (Milosavljević et al. 2007; Springel & Farrar 2007), and at  $R_{200}$ .

We define the pairwise velocity of a satellite cluster,  $\mathbf{V}_c$ , as the velocity of the satellite relative to that of the main cluster,  $\mathbf{V}_c \equiv \mathbf{V}_{\text{main}} - \mathbf{V}_{\text{sat}}$ . When satellite clusters are close to the main cluster,  $V_c$  must be strongly influenced (if not completely determined) by the gravitational potential of the main cluster. Thus,  $V_c$  should depend on the main cluster mass,  $M_{\text{main}}$ . If  $V_c$  is solely determined by the gravitational potential of the main cluster, then  $V_c \propto M_{\text{main}}^{1/2}$ . In reality, however, it is not only the gravity of the main cluster but also the influences from the surrounding large-scale structures that should determine  $V_c$  (Benson 2005; Wang et al. 2005; Wetzel 2010).

Figure 1 shows the distribution of satellite clusters in the  $\log V_c - \log M_{\text{main}}$  plane (dotted line) at  $z = 0$ . There is a clear correlation between  $V_c$  and  $M_{\text{main}}$  (the larger the  $M_{\text{main}}$  is, the larger the  $V_c$  becomes), although it is not simply  $V_c \propto M_{\text{main}}^{1/2}$ . The dotted line in Figure 1 shows the distribution of all satellite clusters. Next, we shall select the satellite clusters that belong to bullet-like systems. We define the bullet-like system as follows: the main cluster exerts dominant gravitational force on satellite clusters, and at least one satellite cluster is on its way to head-on merging with the main cluster. More specifically, the following three criteria are used to select the candidate bullet-cluster systems from the clusters of clusters at a given  $z$ .

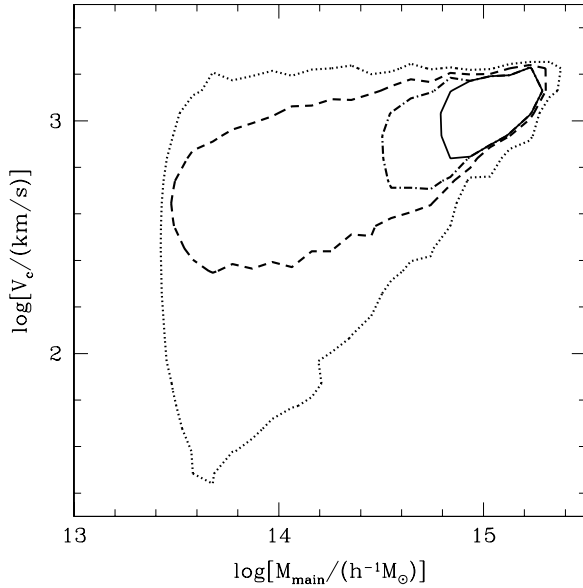


**Figure 1.** Distribution of satellite clusters in the  $V_c$ – $M_{\text{main}}$  plane. The dotted line shows all the satellite clusters found in the simulation at  $z = 0$ ; the dashed line shows those lying between  $2R_{200} \leq r \leq 3R_{200}$  from the main cluster; the dot-dashed line shows those lying between  $2R_{200} \leq r \leq 3R_{200}$  and about to undergo nearly head-on collisions with  $|\cos \theta| \geq 0.9$ ; and the solid line shows those lying between  $2R_{200} \leq r \leq 3R_{200}$ , about to undergo nearly head-on collisions, and having small masses compared to the main cluster mass,  $M_{\text{sat}}/M_{\text{main}} \leq 1/10$ , where  $M_{\text{main}} \geq 0.7 \times 10^{15} h^{-1} M_{\odot}$ .

1. Satellite clusters lie between  $2R_{200} \leq r \leq 3R_{200}$ , and thus their motion is predominantly determined by the gravitational potential of the main cluster.
2. Satellite clusters are about to undergo nearly head-on collisions with the main cluster:  $|\mathbf{V}_c \cdot \mathbf{r}|/(|\mathbf{V}_c||\mathbf{r}|) \geq 0.9$ .
3. The mass of satellites is less than or equal to 10% of that of the main cluster,  $M_{\text{sat}}/M_{\text{main}} \leq 1/10$ , and the main cluster mass is greater than some value,  $M_{\text{main}} \geq M_{\text{crit}}$ .

The third criterion is motivated by the observation of 1E0657-57 indicating that the mass of the bullet subcluster is an order of magnitude lower than that of the massive main cluster, and the mass of the main cluster is  $\sim 10^{15} h^{-1} M_{\odot}$  (Springel & Farrar 2007). As the latest simulation by Mastropietro & Burkert (2008) showed that the mass ratio of 6 : 1 best reproduces the observed data of 1E0657-56 (also see Nusser 2008), we have also studied the case with  $M_{\text{sat}}/M_{\text{main}} \leq 1/5$ , finding similar results; thus, our conclusion is insensitive to the precise value of the mass ratio. In Figures 2 and 3, we show the distribution of the mass ratio,  $M_{\text{sat}}/M_{\text{main}}$ , at  $z = 0$  and 0.5, respectively. As expected, larger- $M_{\text{sat}}/M_{\text{main}}$  (i.e., closer-to-major-merger) collisions are exponentially rare. This makes 1E0657-57 even rarer, if the mass ratio is as large as  $M_{\text{sat}}/M_{\text{main}} = 1/6$ . For the rest of the paper, we shall study the case of  $M_{\text{sat}}/M_{\text{main}} < 1/10$ , keeping in mind that 1E0657-57 can be even rarer than our study indicates.

In Figure 1, we show the distribution of satellite clusters satisfying the condition 1 (dashed line), the conditions 1 and 2 (dot-dashed line), and the conditions 1, 2, and 3 (solid line). Note that  $V_c$  of the satellite clusters that satisfy all of the above conditions approximately follows  $V_c \propto M_{\text{main}}^{1/2}$ . This is an expected result, as the satellite clusters in this case are basically point masses (nearly) freely falling into the main cluster. We also find similar results for  $z = 0.5$ .

In Tables 2 and 3, we show the number of bullet-like systems satisfying all of the above conditions at  $z = 0$  and 0.5,

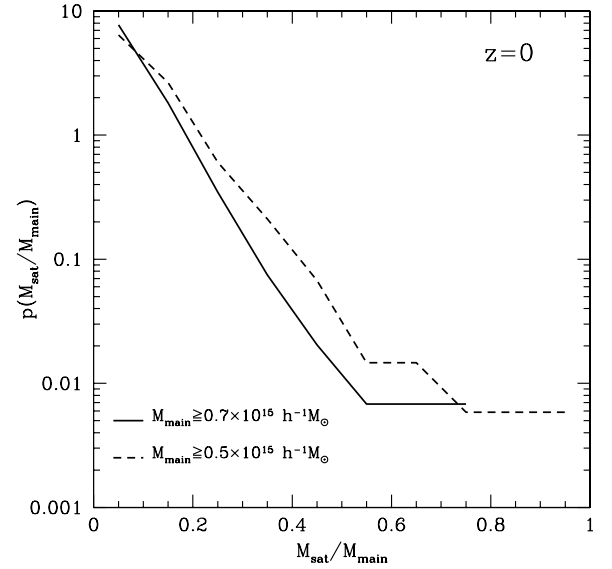


**Figure 2.** Distribution of the sub-main cluster mass ratio,  $M_{\text{sat}}/M_{\text{main}}$ , at  $z = 0$ . The solid and dashed lines show the distribution for the main cluster masses of  $M_{\text{main}} > 0.7$  and  $0.5 \times 10^{15} h^{-1} M_{\odot}$ , respectively. The distribution is normalized to unity when integrated,  $\int_0^1 p(x) dx = 1$ .

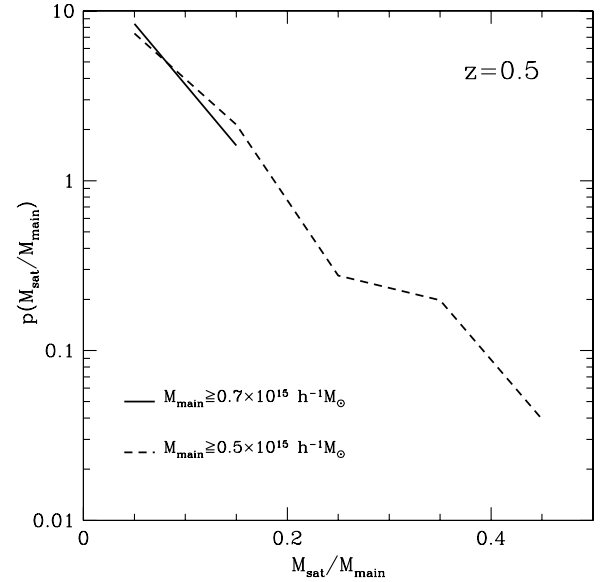


**Figure 3.** Same as Figure 2, but for  $z = 0.5$ .

respectively. At  $z = 0$ , about one in three clusters of clusters with  $M_{\text{main}} \geq 0.7 \times 10^{15} h^{-1} M_{\odot}$  contains a nearly head-on collision subcluster. At  $z = 0.5$ , about one in five clusters of clusters with  $M_{\text{main}} \geq 0.7 \times 10^{15} h^{-1} M_{\odot}$  contains a nearly head-on collision subcluster. Therefore, head-on collision systems are quite common, but what about their infall velocities?

We calculate the probability density distribution of  $\log V_c$  using the selected bullet-like systems (within  $(2-3)R_{200}$ ) at  $z = 0$  and 0.5. The results for  $M_{\text{main}} \geq 0.7 \times 10^{15} h^{-1} M_{\odot}$  are shown in Figures 4 ( $z = 0$ ) and 5 ( $z = 0.5$ ). A striking result seen from Figure 4 is that, of 1135 bullet-like systems shown here for  $z = 0$ , none have an infall velocity as high as  $3000 \text{ km s}^{-1}$ , which is required to explain the X-ray and weak lensing data of 1E0657-56 (Mastropietro & Burkert 2008). A lower velocity,  $2000 \text{ km s}^{-1}$ , is also rare: none (out of 1135) within  $(2-3)R_{200}$  have  $V_c \geq 2000 \text{ km s}^{-1}$  at  $z = 0$ .

**Table 2**  
Bullet-like Systems at  $z = 0$  from the MICE Simulation

$M_{\text{main}}$ ( $10^{15} h^{-1} M_{\odot}$ )	Number of Clusters of Clusters at $z = 0$	Number of Bullet-like Systems <sup>a</sup> at $z = 0$	Number of Bullet-like Systems <sup>b</sup> at $z = 0$
$\geq 0.5$	8523	2189	3093
$\geq 0.7$	3135	1135	1402
$\geq 1$	911	351	391

**Notes.**

<sup>a</sup> For  $M_{\text{sat}}/M_{\text{main}} \leq 1/10$ . A “bullet-like system” is defined as a nearly head-on collision system satisfying all of the conditions (1, 2, and 3) given in Section 3.

<sup>b</sup> For  $M_{\text{sat}}/M_{\text{main}} \leq 1/5$ .

**Table 3**  
Bullet-like Systems at  $z = 0.5$  from the MICE Simulation

$M_{\text{main}}$ ( $10^{15} h^{-1} M_{\odot}$ )	Number of Clusters of Clusters at $z = 0.5$	Number of Bullet-like Systems <sup>a</sup> at $z = 0.5$	Number of Bullet-like Systems <sup>b</sup> at $z = 0.5$
$\geq 0.5$	3108	186	240
$\geq 0.7$	800	78	93
$\geq 1$	138	27	32

**Notes.**

<sup>a</sup> For  $M_{\text{sat}}/M_{\text{main}} \leq 1/10$ .

<sup>b</sup> For  $M_{\text{sat}}/M_{\text{main}} \leq 1/5$ .

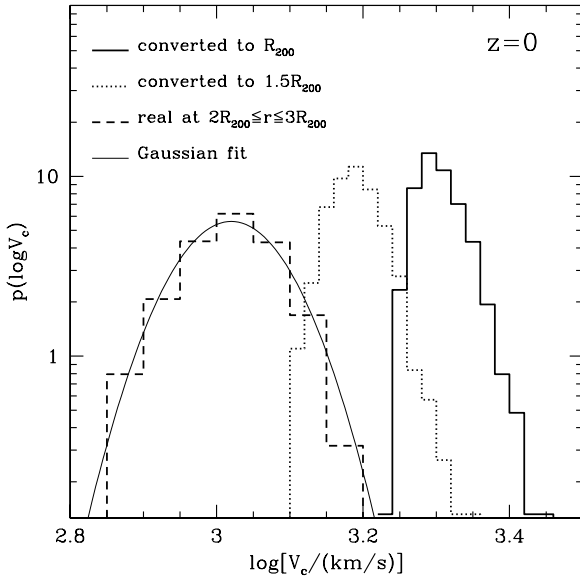


**Figure 4.** Probability density distribution of the infall velocities,  $\log V_c$ , of the bullet-cluster-like systems at  $z = 0$ . The main cluster masses are  $M_{\text{main}} \geq 0.7 \times 10^{15} h^{-1} M_{\odot}$ , for which there are 1135 bullet-like systems in the simulation at  $z = 0$ . The dashed line shows the distribution of  $\log V_c$  within  $2 \leq r/R_{200} \leq 3$  measured from the simulation. This distribution shows that the initial velocities used by Mastropietro & Burkert (2008),  $V_c \geq 2000 \text{ km s}^{-1}$  at  $2.2R_{200}$ , are incompatible with the prediction of a  $\Lambda$ CDM model: none (out of 1135 eligible samples) have a velocity as high as  $V_c \geq 2000 \text{ km s}^{-1}$  in  $2 \leq r/R_{200} \leq 3$ . The dotted and solid lines show the distribution of  $V_c$  at  $1.5R_{200}$  and  $R_{200}$ , respectively, which are obtained by converting the dashed line using Equation (1). We also show a Gaussian fit to the dashed line, which is given by Equation (2). Note that  $10^{3.2} = 1585$ ,  $10^{3.3} = 1995$ , and  $10^{3.4} = 2512$ .

We find a similar result for  $z = 0.5$  (Figure 5): *none* (out of 78) have the infall velocity as high as  $3000 \text{ km s}^{-1}$ , and only one has  $V_c \geq 2000 \text{ km s}^{-1}$ . However, we would need better statistics (i.e., a bigger simulation) at  $z = 0.5$  to obtain more accurate probability. In any case, Mastropietro & Burkert (2008)

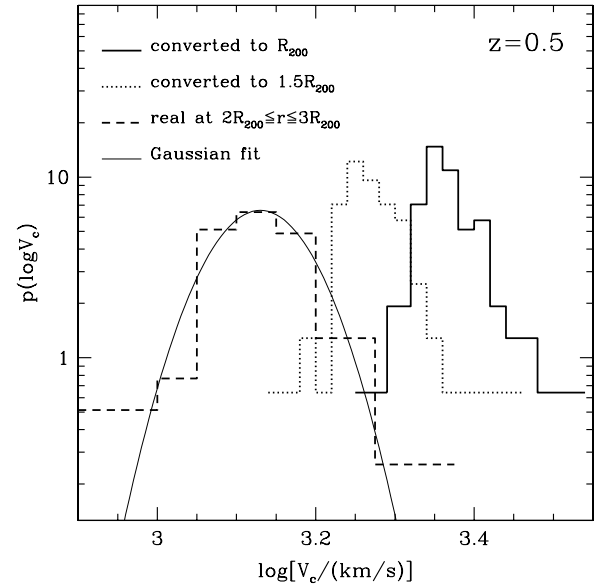


**Figure 5.** Same as Figure 4, but for  $z = 0.5$ . The main cluster masses are  $M_{\text{main}} \geq 0.7 \times 10^{15} h^{-1} M_{\odot}$ , for which there are 177 bullet-like systems in the simulation at  $z = 0.5$ . None have a velocity as high as  $V_c = 3000 \text{ km s}^{-1}$  in  $2 \leq r/R_{200} \leq 3$ , while there is one subcluster with velocity  $V_c \geq 2000 \text{ km s}^{-1}$  in  $2 \leq r/R_{200} \leq 3$ . (This subcluster has  $V_c = 2049 \text{ km s}^{-1}$ .) We also show a Gaussian fit to the dashed line, which is given by Equation (2). Note that  $10^{3.2} = 1585$ ,  $10^{3.3} = 1995$ , and  $10^{3.4} = 2512$ .

argued that an infall velocity of  $2000 \text{ km s}^{-1}$  is not enough to explain the X-ray brightness ratio of the main and subcluster or the X-ray morphology of the main cluster. These results indicate that the existence of 1E0657-56 rules out  $\Lambda$ CDM, unless a lower infall velocity solution for 1E0657-56 is found.

The significance increases if we lower the minimum main cluster mass. Mastropietro & Burkert (2008) argue that  $M_{\text{main}} \sim 0.5 \times 10^{15} h^{-1} M_{\odot}$  fits the data of 1E0657-56 better. For a lower minimum main cluster mass,  $M_{\text{main}} \geq 0.5 \times 10^{15} h^{-1} M_{\odot}$ , none of the 2189 bullet-like systems at  $z = 0$  have  $V_c \geq 2000 \text{ km s}^{-1}$ ,



none of the 186 systems at  $z = 0.5$  have  $V_c \geq 3000 \text{ km s}^{-1}$ , and only one system at  $z = 0.5$  has  $V_c \geq 2000 \text{ km s}^{-1}$ .

To examine whether or not the above results depend on the value of the linking length parameter,  $b$ , of the FoF algorithm used for finding clusters of clusters, we have repeated all the analyses by varying the values of  $b$  from 0.15 to 0.5. We have found similar results at both redshifts, demonstrating that our conclusion is insensitive to the exact values of  $b$  used for the identification of clusters of clusters with the FoF algorithm.

To compare with the initial velocities used by the other simulations (Milosavljević et al. 2007; Springel & Farrar 2007), we need to calculate the infall velocity distribution at  $1.5R_{200}$ . As most of the subclusters are located at  $r \gtrsim 2R_{200}$ , we have much fewer subclusters in  $(1-2)R_{200}$ . (There are only 191 subclusters within  $(1-2)R_{200}$  at  $z = 0$ .) To solve this problem and keep the good statistics, we shall use the following simple dynamical model to convert the results in  $(2-3)R_{200}$  to those at  $1.5R_{200}$  as well as at  $R_{200}$ .

The motion of the subclusters located in  $(2-3)R_{200}$  is predominantly determined by the gravitational potential of the main halo. This is especially true for those in a nearly head-on collision course (i.e., nearly a radial orbit); thus, one may treat a selected sub-main cluster system as an isolated two-body system. Under this assumption, the pairwise velocity at  $r_{\text{in}} < 2R_{200}$  is given in terms of the velocity at  $r_{\text{out}} \geq 2R_{200}$  (which is measured from the simulation) and the mass of the main halo (which is also measured from the simulation):

$$V_c^2(r_{\text{in}}) = V_c^2(r_{\text{out}}) + \frac{2GM_{\text{main}}}{R_{200}} \left( \frac{R_{200}}{r_{\text{in}}} - \frac{R_{200}}{r_{\text{out}}} \right), \quad (1)$$

where  $G = 4.3 \times 10^{-9} \text{ km}^2 \text{ s}^{-2} M_{\odot}^{-1} \text{ Mpc}$  is Newton's gravitational constant.

In Figures 4 and 5, we show the probability density distribution of  $\log V_c$  at  $z = 0$  and  $0.5$ , respectively. The dashed lines show the original distribution for  $(2-3)R_{200}$ , while the dotted and solid lines show the distribution at  $1.5R_{200}$  and  $R_{200}$ , respectively, computed from Equation (1). We find that the initial velocities used by Milosavljević et al. (2007;  $\approx 1600 \text{ km s}^{-1}$ ) and Springel & Farrar (2007;  $\approx 2000 \text{ km s}^{-1}$ ) are consistent with the predictions of a  $\Lambda$ CDM model: at  $1.5R_{200}$ , 9 (out of 1135) subclusters have  $V_c \geq 2000 \text{ km s}^{-1}$  at  $z = 0$ , and 16 (out of 117) subclusters have  $V_c \geq 2000 \text{ km s}^{-1}$  at  $z = 0.5$ . However, these simulations do not reproduce the details of the X-ray and weak lensing data of 1E0567-56 (Mastropietro & Burkert 2008), and thus this agreement does not imply that the existence of 1E0567-56 is consistent with  $\Lambda$ CDM.

How reliable is this extrapolation of the infall velocity? To check the accuracy of Equation (1), we compare  $p(V_c)$  in  $2 \leq r/R_{200} \leq 2.4$  measured from the simulation and  $p(V_c)$  at  $2.2R_{200}$  computed from Equation (1). Specifically, we use Equation (1) to calculate the velocity at  $r_{\text{in}} = 2.2R_{200}$  from velocities in  $2.5R_{200} \leq r_{\text{out}} \leq 3R_{200}$ . In Figure 6, we show the measured  $p(V_c)$  in  $2 \leq r/R_{200} \leq 2.4$  (dashed line), the predicted  $p(V_c)$  at  $2.2R_{200}$  (solid line), and the original  $p(V_c)$  in  $2.5 \leq r/R_{200} \leq 3$  (dotted line). We find an excellent agreement between the measured and predicted distribution.

#### 4. DISCUSSION AND CONCLUSION

Mastropietro & Burkert (2008) showed that the subcluster initial velocity of  $3000 \text{ km s}^{-1}$  at the separation of 5 Mpc is required to explain the X-ray and weak lensing data of 1E0657-56 at  $z = 0.296$ . They argued that a lower velocity,  $2000 \text{ km s}^{-1}$ ,

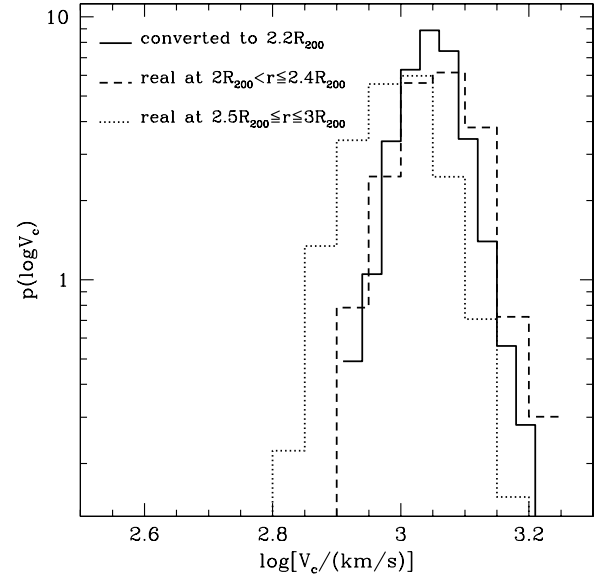


**Figure 6.** Testing Equation (1). The dashed line shows the distribution of  $\log V_c$  in  $2 \leq r/R_{200} \leq 2.4$  measured from the simulation, while the solid line shows the distribution of  $\log V_c$  at  $r_{\text{in}} = 2.2R_{200}$  calculated from the measured distribution in  $2.5 \leq r_{\text{out}}/R_{200} \leq 3$  (dotted line) and Equation (1).

also has to be excluded because it cannot reproduce the observed X-ray brightness ratio of the main and subcluster or the X-ray morphology of the main cluster.

In this paper, we have shown that such a high velocity at 5 Mpc, which is about two times  $R_{200}$  of the main cluster, is incompatible with the prediction of a  $\Lambda$ CDM model. Using the results at  $z = 0$  and  $M_{\text{main}} \geq 0.7 \times 10^{15} h^{-1} M_{\odot}$ ,  $\Lambda$ CDM is excluded by more than 99.91% confidence level (none of the 1135 subclusters have  $V_c \geq 2000 \text{ km s}^{-1}$  in  $2 \leq r/R_{200} \leq 3$ ). For a lower minimum main cluster mass,  $M_{\text{main}} \geq 0.5 \times 10^{15} h^{-1} M_{\odot}$ ,  $\Lambda$ CDM is excluded by more than 99.95% confidence level (none of the 2189 subclusters have  $V_c \geq 2000 \text{ km s}^{-1}$  in  $2 \leq r/R_{200} \leq 3$ ).

The results at  $z = 0.5$  are not yet fully conclusive due to the limited statistics: none of the 78 subclusters have  $V_c \geq 3000 \text{ km s}^{-1}$  in  $2 \leq r/R_{200} \leq 3$ , while there is one subcluster with  $V_c \geq 2000 \text{ km s}^{-1}$  in  $2 \leq r/R_{200} \leq 3$ . For  $M_{\text{main}} \geq 0.5 \times 10^{15} h^{-1} M_{\odot}$ , none of the 186 subclusters have  $V_c \geq 3000 \text{ km s}^{-1}$ , while there is one subcluster with  $V_c \geq 2000 \text{ km s}^{-1}$ .

While these confidence levels are directly measured from the simulation, one can estimate the probability better by fitting the probability density,  $p(\log V_c)$ , to a Gaussian distribution as

$$p(\log V_c) = \frac{1}{\sqrt{2\pi}\sigma_v} \exp \left[ -\frac{(\log V_c - \nu)^2}{2\sigma_v^2} \right], \quad (2)$$

where  $V_c$  is in units of  $\text{km s}^{-1}$  and  $\nu$  and  $\sigma_v$  are the two fitting parameters. The best-fit values of the two parameters for  $z = 0$  and  $0.5$  are  $(\nu, \sigma_v) = (3.02, 0.07)$  and  $(3.13, 0.06)$ , respectively. The mean velocity at  $z = 0$  is smaller than that at  $z = 0.5$  by a factor of  $10^{3.13-3.02} = 1.29$ . This may be understood as the effect of  $\Lambda$  slowing down the structure formation at  $z < 0.5$ .

Generally, one has to be careful about this approach, as we are probing the tail of the distribution, where the above fits may not be accurate. Using the above Gaussian fits, we find  $P(> 3000 \text{ km s}^{-1}) = 3.3 \times 10^{-11}$  and  $3.6 \times 10^{-9}$  at  $z = 0$  and  $0.5$ , respectively. We also find  $P(> 2000 \text{ km s}^{-1}) = 2.9 \times 10^{-5}$  and  $2.2 \times 10^{-3}$  at  $z = 0$  and  $0.5$ , respectively. These numbers

pose a serious challenge to  $\Lambda$ CDM, unless one finds a lower velocity solution for 1E0657-56. Here, a “lower velocity” may be somewhere between  $V_c \lesssim 1500$  and  $1800 \text{ km s}^{-1}$  at  $r \sim 2R_{200}$ , which give 1% probabilities at  $z = 0$  and  $z = 0.5$ , respectively.

The bullet cluster 1E0657-56 is not the only site of violent cluster mergers. For example, there are A520 (Markevitch et al. 2005) and MACS J0025.4-1222 (Bradač et al. 2008). Also, high-resolution mapping observations of the Sunyaev-Zel’dovich (SZ) effect have revealed a violent merger event in RX J1347-1145 at  $z = 0.45$  (Komatsu et al. 2001; Kitayama et al. 2004; Mason et al. 2010), which are confirmed by X-ray observations (Allen et al. 2002; Ota et al. 2008). The shock velocity inferred from the SZ effect and the X-ray data of RX J1347-1145 is  $4600 \text{ km s}^{-1}$  (Kitayama et al. 2004), which is similar to the shock velocity observed in 1E0657-56 (Markevitch 2006). The lack of structure in the redshift distribution of member galaxies of RX J1347-1145 suggests that the geometry of the merger of this cluster is also closer to edge-on (Lu et al. 2010). However, the lack of a bow shock in the *Chandra* image may suggest that it is not quite as edge-on as 1E0657-56. In any case, it seems plausible that there may be more clusters like 1E0657-56 in our universe. This too may present a challenge to  $\Lambda$ CDM.

Since the volume of the MICE simulation is close to the Hubble volume,<sup>4</sup> our results can be compared directly with observations, provided that detailed follow-up observations are available for us to calculate the shock velocity, gas distribution, and dark matter distribution. These three observations would then enable us to estimate the mass ratio and initial velocity of the collision which, in turn, can be compared to the probability distribution we have derived in this paper. Note also that the probabilities obtained in our work are the conditional ones. That is, the probability for which a fitting formula is provided is the probability of the velocity of bullet systems that are nearly head-on, with 1:10 or more mass ratio, and with  $M_{\text{main}} \geq 0.7 \times 10^{15} h^{-1} M_{\odot}$ . If we computed the probability of finding high-velocity bullet systems among all clusters from the simulation, then the probability would be even smaller than those estimated above. Such a conditional probability is relevant to the observation, if we have sufficient amount of data for estimating the mass ratio and the initial velocity, as mentioned above. Note that we have precisely such data for 1E0657-56.

An interesting question that we have not addressed in this paper is how many high-velocity bullet systems are expected for flux-limited galaxy cluster surveys, such as the South Pole Telescope and eROSITA (extended ROentgen Survey with an Imaging Telescope Array). To calculate, e.g.,  $dN_{\text{bullet}}/dz$ , one needs the light-cone output of the MICE simulation. While we have not investigated this, we expect two major light-cone effects on the infall velocity distribution. First, the infall velocities at high  $z$ ’s should be larger since the effect of  $\Lambda$  has yet to kick in at high  $z$ ’s, which we have already demonstrated here by comparing the mean infall velocity at  $z = 0$  and  $0.5$ . Second, the massive bullet systems with mass greater than  $10^{15} h^{-1} M_{\odot}$  are very rare at higher  $z$ ’s. The first effect will make the high-velocity system more common, while the

second effect will make the high-velocity system less common. In order to quantify the net effect, one needs the light-cone output. However, the light-cone effect alone would not be able to reconcile the existence of 1E0657-56 with the prediction of  $\Lambda$ CDM.

We acknowledge the use of data from the MICE simulations that are publicly available at <http://www.ice.cat/mice>. We thank C. Mastropietro, M. Milosavljević, and P. R. Shapiro for discussions. We also thank an anonymous referee for helpful comments. J.L. is very grateful to the members of the Texas Cosmology Center of the University of Texas at Austin for the warm hospitality during the period of her visit when this work was initiated and performed. J.L. acknowledges the financial support from the Korea Science and Engineering Foundation (KOSEF) grant funded by the Korean Government (MOST, No. R01-2007-000-10246-0). This work is supported in part by the NASA grant NNX08AL43G and the NSF grant AST-0807649.

## REFERENCES

- Allen, S. W., Schmidt, R. W., & Fabian, A. C. 2002, *MNRAS*, **335**, 256  
 Barrena, R., Biviano, A., Ramella, M., Falco, E. E., & Seitz, S. 2002, *A&A*, **386**, 816  
 Benson, A. J. 2005, *MNRAS*, **358**, 551  
 Bradač, M., Allen, S. W., Treu, T., Ebeling, H., Massey, R., Morris, R. G., von der Linden, A., & Applegate, D. 2008, *ApJ*, **687**, 959  
 Clowe, D., Bradač, M., Gonzalez, A. H., Markevitch, M., Randall, S. W., Jones, C., & Zaritsky, D. 2006, *ApJ*, **648**, L109  
 Clowe, D., Gonzalez, A., & Markevitch, M. 2004, *ApJ*, **604**, 596  
 Crocce, M., Fosalba, P., Castander, F. J., & Gaztanaga, E. 2010, *MNRAS*, **403**, 1353  
 Davis, M., Efstathiou, G., Frenk, C. S., & White, S. D. M. 1985, *ApJ*, **292**, 371  
 Farrar, G. R., & Rosen, R. A. 2007, *Phys. Rev. Lett.*, **98**, 171302  
 Fosalba, P., Gaztañaga, E., Castander, F. J., & Manera, M. 2008, *MNRAS*, **391**, 435  
 Hayashi, E., & White, S. D. M. 2006, *MNRAS*, **370**, L38  
 Kitayama, T., Komatsu, E., Ota, N., Kuwabara, T., Suto, Y., Yoshikawa, K., Hattori, M., & Matsuo, H. 2004, *PASJ*, **56**, 17  
 Komatsu, E., et al. 2001, *PASJ*, **53**, 57  
 Komatsu, E., et al. 2010, *ApJS*, submitted (arXiv:1001.4538)  
 Lu, T., et al. 2010, *MNRAS*, **403**, 1787  
 Lukić, Z., Reed, D., Habib, S., & Heitmann, K. 2009, *ApJ*, **692**, 217  
 Markevitch, M. 2006, in *Proc. X-Ray Universe 2005*, ed. A. Wilson (ESA SP-604; Noordwijk: ESA), 723  
 Markevitch, M., Gonzalez, A. H., Clowe, D., Vikhlinin, A., Forman, W., Jones, C., Murray, S., & Tucker, W. 2004, *ApJ*, **606**, 819  
 Markevitch, M., Gonzalez, A. H., David, L., Vikhlinin, A., Murray, S., Forman, W., Jones, C., & Tucker, W. 2002, *ApJ*, **567**, L27  
 Markevitch, M., Govoni, F., Brunetti, G., & Jerius, D. 2005, *ApJ*, **627**, 733  
 Mason, B. S., et al. 2010, *ApJ*, **716**, 739  
 Mastropietro, C., & Burkert, A. 2008, *MNRAS*, **389**, 967  
 Milosavljević, M., Koda, J., Nagai, D., Nakar, E., & Shapiro, P. R. 2007, *ApJ*, **661**, L131  
 Nusser, A. 2008, *MNRAS*, **384**, 343  
 Ota, N., et al. 2008, *A&A*, **491**, 363  
 Springel, V. 2005, *MNRAS*, **364**, 1105  
 Springel, V., et al. 2005, *Nature*, **435**, 629  
 Springel, V., & Farrar, G. R. 2007, *MNRAS*, **380**, 911  
 Takizawa, M. 2005, *ApJ*, **629**, 791  
 Takizawa, M. 2006, *PASJ*, **58**, 925  
 Wang, H. Y., Jing, Y. P., Mao, S., & Kang, X. 2005, *MNRAS*, **364**, 424  
 Warren, M. S., Abazajian, K., Holz, D. E., & Teodoro, L. 2006, *ApJ*, **646**, 881  
 Wetzel, A. R. 2010, *MNRAS*, submitted (arXiv:1001.4792)

<sup>4</sup> For example, the comoving volume available from  $z = 0$  to  $z = 1$  over the full sky is  $54 h^{-3} \text{ Gpc}^3$ , which is only twice as large as the volume of the MICE simulation. The comoving volume out to  $z = 3$  is still  $396 h^{-3} \text{ Gpc}^3$ , which is nowhere near enough to overcome the probability of  $10^{-9}$ .